Tuning the 4*f* state occupancy of Ce in highly correlated CeSi/Fe multilayers: An x-ray absorption spectroscopy study

M. Münzenberg*
IV. Physikalisches Institut, Universität Göttingen, Friedrich-Hund-Platz 1, 37077 Göttingen, Germany

W. Felsch
I. Physikalisches Institut, Universität Göttingen, Friedrich-Hund-Platz 1, 37077 Göttingen, Germany

P. Schaaf
II. Physikalisches Institut, Universität Göttingen, Friedrich-Hund-Platz 1, 37077 Göttingen, Germany
(Received 15 August 2006; revised manuscript received 29 May 2007; published 23 July 2007)

Spectra of x-ray absorption were measured at the $L_{2,3}(2p)$ and $M_{4,5}(3d)$ edges of Ce in multilayers $[Ce_{1-x}Si_x/Fe]xn$ (x between 0.1 and 0.65), with single-phase amorphous $Ce_{1-x}Si_x$ sublayers. The study uncovers the highly correlated nature of this layered system; an α-phase-like electronic configuration of Ce is observed, which indicates considerable hybridization between the 4*f* and conduction-band states. This is at variance with single alloy films $Ce_{1-x}Si_x$ which show a γ-phase-like Ce configuration already at $x=0.1$. X-ray magnetic circular dichroism measured at the $L_{2,3}$ edges of Ce in the multilayers reveals magnetic order on the 5*d* electrons, induced by the interaction with Fe at the interfaces. With increasing the Si content, the strength of the 4*f*-conduction-band hybridization is reduced, which is reflected in a growing occupation of the Ce 4*f* states. Variations of the line shape and intensity of the $L_{2,3}$-edge dichroism spectra are very complex. The spectra not only are related to the magnetic 5*d* polarization in the ground state but are largely controlled by the exchange interaction between the photoexcited 5*d* electron and the 4*f* electron, which generates a spin-dependent enhancement of the radial parts of the 2*p*-to-5*d* matrix element. The strength of the 4*f*-5*d* exchange interaction can be controlled by varying the composition of the $Ce_{1-x}Si_x$ sublayers. At high Si concentration and low temperature, it induces a change in sign of the dichroic signal. We present a detailed discussion within a simple phenomenological model.

DOI: 10.1103/PhysRevB.76.014427 PACS number(s): 75.70.Cn, 78.67.Pt, 78.70.Dm, 71.27.+a

I. INTRODUCTION

There is broad consensus that the unusual properties of Ce and its compounds originate essentially from the interplay of strong correlations between the Ce 4*f* electrons and hybridization between 4*f*- and conduction-electron states. Phenomena such as intermediate valency, pointing to noninteger occupation of the 4*f* shell, or heavy-fermion behavior, characterized by an extremely large contribution of the electronic specific heat, are prominent observations on such systems. Perhaps one of the most intriguing phenomena is the γ-α phase transition in Ce metal.[1] It occurs under pressure at room temperature or, at ambient pressure, on cooling to low temperature. Complexity of the underlying mechanisms is reflected in the lattice-symmetry preserving collapse of the atomic volume by about 15%, the loss of the magnetic moment, and a profound modification of the electronic structure. The transition is driven by a sensible increase of the hybridization between 4*f*- and conduction-electron states, which leads to a delocalization of the 4*f* states in the α phase.[2,3] Formally, hybridization may be defined in terms of a configuration interaction. This means that the ground state of Ce is written as a linear combination of $|4f^0v^{n+1}\rangle$, $|4f^1v^n\rangle$, and $|4f^2v^{n-1}\rangle$ electronic states (v stands for the valence electrons), i.e., in terms of differently occupied 4*f* states. In compounds, Ce shows γ- or α-phase-like character, depending of the hybridization strength. In α-like compounds such as $CeFe_2$ or $CeCo_5$, the Ce atoms carry an ordered magnetic moment,[4] in contradistinction to elemental α-phase Ce metal.[1]

There is an ongoing interest in the electronic structure of the intermetallic compounds $CeSi_2$ and CeSi in the context of intermediate-valency, Kondo-lattice, and heavy-fermion phenomena. Most of the information comes from various high-energy spectroscopies with high resolution.[5–8] In these compounds, weak hybridization occurs between the 4*f* and conduction-band states, preferentially with those of *p* symmetry derived from Si. The Ce $|4f^1v^n\rangle$ state dominates the ground-state electronic configuration, with a small admixture of the $|4f^0v^{n+1}\rangle$ state.[7,8] A delicate balance between the Kondo effect quenching the localized 4*f* magnetic moments and the Rudermann-Kittel-Kasuya-Yosida (RKKY) interaction between these moments and the conduction electrons allows for nonmagnetic or magnetically ordered ground states; the former is realized in $CeSi_2$,[9] the latter in CeSi.[8,10] In a simple picture,[11] this competition is governed by a single parameter, the effective exchange interaction J between the 4*f* and conduction electrons which enters the characteristic energy scales both for the Kondo and RKKY interactions. In turn, J depends on the 4*f*-conduction-band hybridization strength which varies sensitively with the interatomic distances. The fragile character of the weakly hybridized electronic ground-state configuration of Ce in $CeSi_2$ is apparent in the behavior of off-stoichiometric $CeSi_{2-\delta}$ which orders magnetically at $\delta > 0.16$.[12,13] Experiments on single-phase amorphous films of $Ce_{1-x}Si_x$ alloys have shown that struc-

tural disorder stabilizes the γ-like electronic configuration of Ce, on a large scale of Si concentrations $0.2 \leqslant x \leqslant 0.9$.[14] Apparently, the loss of the lattice periodicity reduces the (already weak) $4f$-p hybridization. It is interesting to note that amorphous $Ce_{0.33}Si_{0.67}$ films and the bulk crystalline counterpart $CeSi_2$ present essentially the same local environment around the Ce ions.[15] A study on bulk amorphous $Ce_{1-x}Si_x$ alloys revealed Kondo behavior at low temperature in a wide range of Si concentrations, i.e., the absence of magnetic order and an enhanced electronic specific heat, similar as in heavy-fermion systems.[16] In contrast, Ce shows an α-like electronic configuration in amorphous $Ce_{1-x}Fe_x$ alloy films and a magnetically ordered ground state. In this system, the (itinerant) Ce $4f$ states are strongly hybridized with the Fe $3d$ states.[17] For example, in amorphous $Ce_{0.34}Fe_{0.66}$ the strong hybridization of the corresponding compound $CeFe_2$ is preserved in spite of the structural disorder. Differences in the physical properties are related to the different local structures.

We have previously shown by x-ray absorption spectroscopy (XAS)[18] and studies of x-ray magnetic circular dichroism (XMCD)[18,19] and of resonant x-ray magnetic scattering[20] that the α-phase-like electronic structure of Ce is stabilized in Ce/Fe multilayers on a considerable depth scale near the interface and, in this configuration, carries an ordered magnetic moment on its $4f$ and $5d$ states. Both the stabilization of α-like Ce and its magnetic polarization are driven by interface effects, i.e., by in-plane elastic strain resulting from the large mismatch between the interatomic spacings at the interfaces of the Ce and Fe layers and by strong interfacial electronic correlations between the Ce $4f$ and $5d$ states and the Fe $3d$ states,[17–19,21,22] respectively. Subsequent experiments have shown that the absorption of hydrogen in the Ce sublayers reduces the $4f$-state conduction-band hybridization and leads to a relocalization of the $4f$ states; i.e., the γ-phase-like electronic configuration of Ce is stabilized in multilayers $CeH_{2-\delta}$/Fe due to an expansion of the Ce-ion interatomic distance in the $CeH_{2-\delta}$ lattice. The result is a profound modification of the electronic and magnetic properties.[23–26] The magnetization of the hydrided layers, for example, turns perpendicular to the layer plane at low temperatures. The orientational transition involves the Ce $4f$ moments at the interfaces interacting with the Fe $3d$ states via the Ce $5d$ states.[23,24] The XMCD spectra probing the $5d$ states show very unusual temperature- and orientation-dependent line shapes.[27]

Here, we report on an experimental XAS study of the electronic and magnetic properties of multilayers combining amorphous $Ce_{1-x}Si_x$ with bcc Fe. It was conceived, with the very different properties of the Ce/Fe and $CeH_{2-\delta}$/Fe multilayers in mind, to explore the effects of a progressive transition of the Ce $4f$ states from itinerancy in the α phase (strongly hybridized) to localization in the γ phase (weakly hybridized), simply controlled by introducing an increasing amount of the (s,p) element Si into the Ce sublayers in the Ce/Fe heterostructures. In fact, according to the experiments on thin $Ce_{1-x}Si_x$ films mentioned above, ~20% of Si would stabilize the γ-phase-like electronic structure of Ce.[14] The single-phase nature of the amorphous $Ce_{1-x}Si_x$ sublayers makes the multilayers well suited for such study. We note that a gradual transition between the two Ce configurations by hydrogenation of Ce is not experimentally achievable: the primary solubility of H in Ce is very small, so the phase $CeH_{2-\delta}$ is preferred. We found that in the multilayer environment with Fe, the Ce $4f$ states in $Ce_{1-x}Si_x$ are more strongly hybridized with the conduction-band states than in the bare alloy layers. Even at Si concentrations as high as 65%, an important hybridization is still perceptible: Ce presents the α-phase-like configuration, even though the occupation of the $4f$ states is high. This is in contrast to the bare layers. It points to a stabilization by in-plane elastic strain at the interfaces and to involvement of the Ce $5d$ and Fe $3d$ states in the hybridization process with the $4f$ states. As in the Si-free layered Ce/Fe system, the α-like Ce phase is magnetically ordered. The observation once again illustrates the sensitivity of the $4f$ configuration in Ce systems to surface and interface effects, caused by modifications of the nature and strength of their hybridization with the electronic environment.[28] To explore this behavior, it is important to obtain information on the correlation between the Ce $5d$, Ce $4f$, and Fe $3d$ electrons in this layered system. This is the intention of the present study.

As in the previous work on the Ce-based multilayers,[17,18] a study of XAS at the $M_{4,5}$ and $L_{2,3}$ edges of Ce and of XMCD at the Ce-$L_{2,3}$ edges was systematically performed to explore the ground-state electronic properties of Ce in these multilayers, related to the $4f$ and $5d$ electrons. Particular attention was focused on the $L_{2,3}$-edge spectra that provide information on the $5d$-electron states. This is crucial in understanding the magnetic properties of the multilayers since the Ce $5d$ electrons play a key role in the subtle exchange process between the Fe $3d$ and Ce $4f$ magnetic moments. In addition, Ce L-edge XAS is a well-suited technique to help clarify the electronic ground-state configuration of Ce because under the influence of the $4f$-electron core-hole Coulomb interaction the signatures of the mainly $|2\underline{p}4f^0\upsilon^{n+2}\rangle$ and $|2\underline{p}4f^1\upsilon^{n+1}\rangle$ final states (underscore signifies a hole state) are well separated in the spectra.

The paper is organized as follows. In Sec. II, we present details of the experiments performed as well as basic characteristics of the multilayer samples. We discuss the results of ^{57}Fe Mössbauer spectroscopy which supplements the XMCD data. In Sec. III, we present and discuss the XAS (III A) and XMCD (III B) data. Section III A shows that by varying the Si concentration in the $Ce_{1-x}Si_x$ sublayers, the occupancy of the Ce $4f$ states may be tailored. In Sec. III B, we discuss the mechanisms underlying the magnetic polarization of the Ce $4f$ and $5d$ states. We present a phenomenological model of the Ce-$L_{2,3}$-edge XMCD spectra which shows that, at high Si content, their shape and amplitude are strongly influenced by the $4f$-$5d$ exchange interaction.

II. EXPERIMENTAL DETAILS AND SAMPLE CHARACTERISTICS

Multilayers composed of the structural periods $[Ce_{1-x}Si_x(t\ \text{Å})/Fe(30\ \text{Å})]$ and alloy films $Ce_{1-x}Si_x$ were grown by computer-controlled ion-beam sputtering in an ultrahigh vacuum chamber (base pressure $p < 5 \times 10^{-10}$ mbar).

Highly pure sputtering gas Ar (6*N*) and target metals Ce (3*N*) and Fe (4*N*8) were used. The Ce-Si target was composed of a Ce plate partly covered by a 0.5 mm thick Si wafer with a regular array of holes with diameters adapted to the desired concentration of the $Ce_{1-x}Si_x$ films. The actual composition of these films was determined after preparation by Rutherford backscattering spectrometry, with an uncertainty of 2%. Partial pressures of reactive gases (e.g., O_2, N_2, H_2O) were below 10^{-10} mbar during the deposition process. Typical growth rates were 0.5–1.0 Å/s. Deposition was performed at liquid nitrogen temperature to minimize diffusion. For the multilayers, Kapton (12 μm) or Mylar foil (1.5 μm) coated with a 40 Å thick Cr buffer layer was used as substrate for the x-ray absorption experiments to permit measurements in transmission mode, both in the hard and soft x-ray regime, respectively. Multilayer samples for x-ray diffraction, magnetometry, and Mössbauer spectroscopy and individual $Ce_{1-x}Si_x$ alloy films for comparative absorption measurements with hard x rays were deposited on Si (100) wafers; they were equally precoated with a Cr buffer to warrant identical growth conditions and properties of the sample layers. Relaxation of stress in the samples deposited on the Kapton or Mylar foil substrates can be excluded since such stress is dominated by the internal interfaces of the multilayers. The total thickness of the samples was near 4000 Å for the absorption measurements with hard x rays at the Ce *L* edges. In the case of the soft x-ray experiments at the Ce $M_{4,5}$ edges it was important to keep the multilayers sufficiently thin; a total thickness of 150 Å was chosen for the Ce part of the samples in order to have about 50% of transmission. All samples were covered with a 80 Å thick protection layer of Cr.

Structural characterization of the multilayers was performed by x-ray diffraction in $\Theta/2\Theta$ reflection geometry at small and large angles. In the small-angle regime, sharp superlattice Bragg peaks appear up to the sixth order. Analysis of the data employing Parratt fits[29] yields a rms structural roughness of nominally about one monolayer at the interfaces, independent of the $Ce_{1-x}Si_x$ sublayer thickness [we recall that the Fe-layer thickness is always the same (30 Å)]. This shows that the layered stacks are well defined with good periodicity and sharp composition profiles, in agreement with the previous observation on Ce/Fe multilayers.[30] The large-angle diffraction spectra show that the 30 Å thick Fe sublayers grow in the bcc structure without texture. Application of the Debye-Scherrer formula yields a crystallite size of up to 26–30 Å in the growth direction, which corresponds to the film thickness. The $Ce_{1-x}Si_x$ sublayers are amorphous with α-phase-like Ce: there is a broad diffraction maximum near the (111) reflection expected for α-Ce. The single $Ce_{1-x}Si_x$ films grow equally in an amorphous structure, but in this case the position of the broad diffraction maximum indicates γ-phase-like Ce.

As previously shown for the Ce/Fe system,[21] information on the interfacial interaction in the $Ce_{1-x}Si_x$/Fe multilayers can be derived by ^{57}Fe Mössbauer spectroscopy; it supplements the results of x-ray absorption presented below. Figure 1 shows such spectra for three samples with different Si concentrations measured by conversion-electron detection at room temperature. They are magnetically split, according to

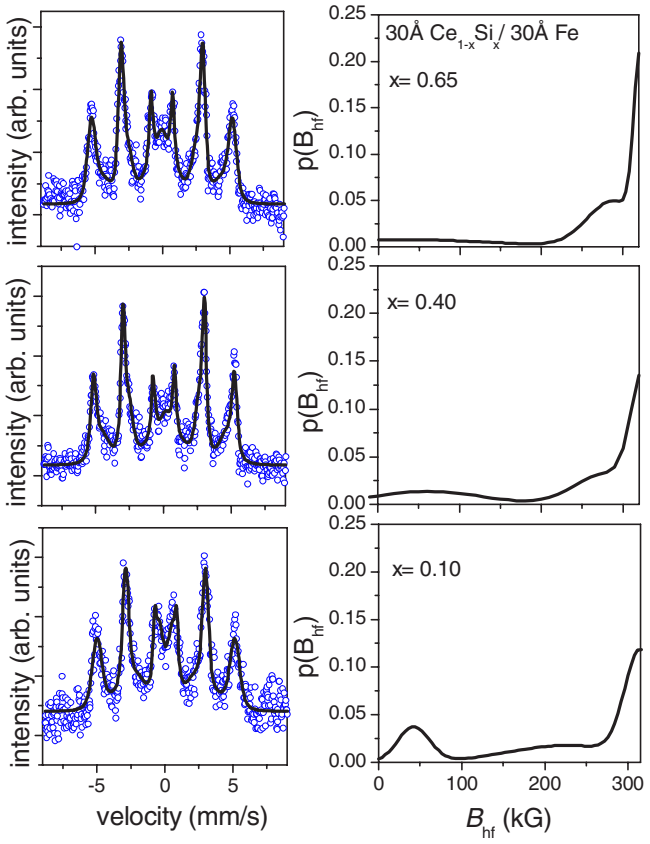

FIG. 1. (Color online) Left: ^{57}Fe Mössbauer conversion-electron spectra at room temperature of multilayers $Ce_{1-x}Si_x$/Fe with different Si concentrations *x*. Solid lines: Fits described in the text. Right: Magnetic hyperfine-field distribution $p(B_{hf})$ corresponding to the contribution of the interfaces to the spectra.

the ferromagnetic nature of the layers. The asymmetry of the lines and the broad background feature in the middle of the spectra indicate the presence of nonequivalent Fe sites. Data analysis was performed as previously, using a model suited to the layered structure of the samples:[21] the spectra were decomposed into a sextet representing the normal bcc part in the core of the Fe layers and a probability distribution of magnetic hyperfine fields attributed to Fe affected by the interfaces, $p(B_{hf})$.[31] These interfacial distributions $p(B_{hf})$ are compared on the right part of Fig. 1. For each multilayer, the contribution of the interface component to the total intensity of the spectrum corresponds to a nominal Fe-layer thickness of 8–10 Å per interface, depending on the Si concentration. This corroborates the previous observation on Ce/Fe multilayers.[21] It signifies a sizable magnetic interaction of Fe with Ce and/or Si on a length scale exceeding the local thickness fluctuations derived from the small-angle x-ray diffraction data and mirrors a modification of the electronic structure of Fe near the interfaces. The hyperfine-field distributions underlying the interface component, $p(B_{hf})$, present characteristic structures. As argued before,[21] these structures may be assigned to different parts of the interface. The region at low fields ($B_{hf} < 150$ kG) represents Fe atoms next to the interface. For the multilayer with $x=0.1$, there is a pronounced maximum at $B_{hf}=45$ kG. Here, the low-field

part of $p(B_{hf})$ corresponds to 2.5 Å per interface, i.e., to nominally one monolayer of Fe. This value is compatible with the structural rms roughness. As previously for the Ce/Fe multilayers, we attribute this feature to a weakly magnetic "interface alloy."[21] The low-B_{hf} signature in $p(B_{hf})$ becomes increasingly broader for a growing Si content. It suggests an increasing influence of Si p states on the interfacial interaction in the multilayers. We note that for the highest Si concentration, $x=0.65$, a symmetric doublet has to be added to get a close fit of the Mössbauer spectrum. It indicates the presence of a small amount of paramagnetic Fe in this multilayer (1.5 Å per interface) and may point to the formation of a nonmagnetic silicide. The Mössbauer spectra, as well as the x-ray diffraction data, exclude the formation of Fe silicides (which usually form very easily) on a large depth scale in the Fe sublayers. This must be due to the presence of Ce. The average magnetic hyperfine field at the Fe sites in the $Ce_{1-x}Si_x$/Fe multilayers resulting from the total Mössbauer spectra is reduced by ~22% with respect to the bulk α-Fe value (334 kOe), which confirms the previous result on the Ce/Fe multilayers.[21]

The x-ray absorption spectra of the multilayers were measured in transmission mode, both on the energy-dispersive spectrometer D11 of the DCI storage ring [$L(2p)$ edges of Ce] and on the beamline SU22 on the asymmetric wiggler of the Super-ACO storage ring [$M_{4,5}(3d)$ edges of Ce] at LURE (Orsay, France). Ce-L_3-edge absorption of single $Ce_{1-x}Si_x$ alloy films were recorded on the LURE DCI beamline D42 in the total-electron-yield mode. D11 is equipped with a bent Si(111) crystal selecting an energy band of up to ~250 eV above a chosen absorption edge from the bending-magnet source, with a resolution of 0.3–0.5 eV in the energy range of 5–9 keV. An array of photodiodes acts as a position-sensitive detector. Energies at the beamlines SU22 and D42 are selected by a Beryll(10-10) double-crystal (SU22) and a Si(331) channel-cut monochromator (D42), with resolutions of 0.2–0.3 eV in the energy range 860–930 eV and of 0.3–0.5 eV in the range 5.6–6.3 keV, respectively.

XMCD spectra were measured at the Ce-L_2 and -L_3 edges only (beamline D11), at constant beam helicity, by varying the photon energy across each absorption edge in a single shot. They were recorded at 0.3 mrad below the position of the orbit plane, where the light is circularly polarized to 70%, for two opposite directions of a magnetic field up to 20 kOe, H_+ and H_-, oriented parallel and opposite to the x-ray propagation direction. A high sensitivity of small differences in intensity of the x-ray absorption spectra, typically of 10^{-3}, was achieved by successive accumulation of more than 100 spectra. The magnetic field was applied at grazing incidence (30°) with respect to the layer planes and was high enough to saturate the magnetization of the samples. If $\mu^-(H_{+,-})$ represents the normalized absorption coefficients for right-circularly polarized photons (helicity $-\hbar$) and for the two opposite magnetic fields H_+ and H_-, the XMCD signal is defined as $\Delta\mu=\mu^-(H_+)-\mu^-(H_-)$, according to the generally accepted convention. All XMCD spectra presented here were scaled to 100% circular polarization. They represent an average over the $Ce_{1-x}Si_x$ sublayers. Limited sublayer thicknesses were investigated. It was outside the scope of this study to explore the depth of the Fe-induced magnetic polarization in the $Ce_{1-x}Si_x$ sublayers near the interfaces. Details of the data collection and the experimental setup are described elsewhere.[32,33]

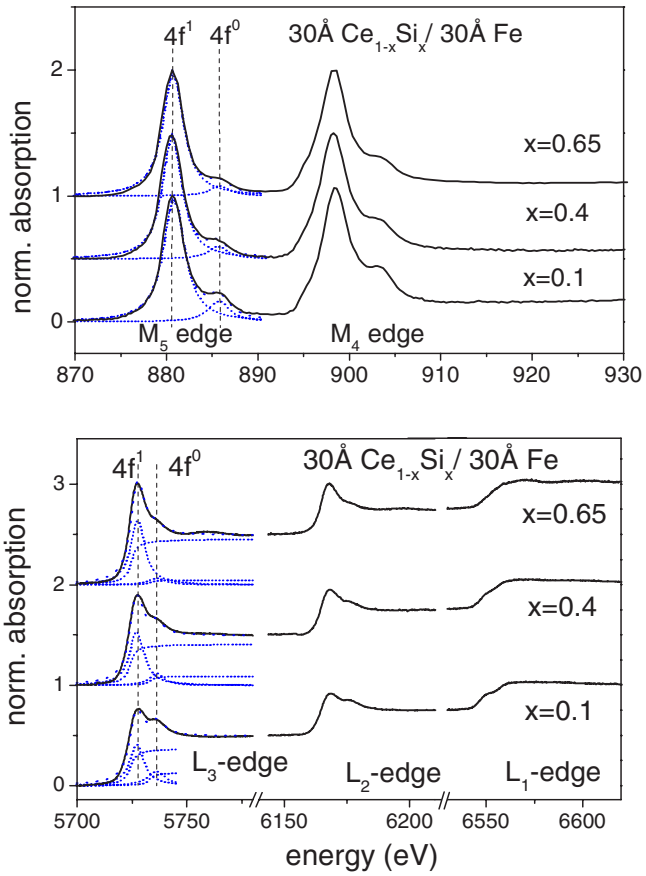

FIG. 2. (Color online) X-ray absorption spectra at the $M_{4,5}$ (top) and $L_{1,2,3}$ (bottom) edges of Ce in multilayers $Ce_{1-x}Si_x$/Fe with different Si concentrations x (detection in transmission). The M-edge spectra are normalized to the amplitude of the M_5-edge spectra arbitrarily set to unity. For the L-edge spectra, the edge jumps are normalized to 0.5 at the L_3 and to 0.25 at the L_2 and L_1 edges, yielding a total jump of 1. The decomposition of the spectra is demonstrated by the superposition of two Lorentzians (M_5 edge, top, blue dotted lines) and of two arctangent functions together with two Lorentzians (L_3 edge, bottom, blue dotted lines). The $4f^1$ and $4f^0$ initial channels are indicated for the M_5 and L_3 edges by the vertical dashed lines.

III. RESULTS AND DISCUSSION

A. Isotropic x-ray absorption spectroscopy: Variation of the Ce 4*f* state occupancy

The $4f$ electronic configuration of Ce in bulk compounds has been extensively investigated by XAS at the $2p\rightarrow 5d$ ($L_{2,3}$) and $3d\rightarrow 4f$ ($M_{4,5}$) excitation thresholds. Recent examples concerning the intermetallic $CeSi_2$ can be found in Refs. 6 and 7. Figure 2 shows the Ce-$L_{1,2,3}$ and $M_{4,5}$-edge spectra of multilayers $[Ce_{1-x}Si_x/Fe]xn$ with different Si concentrations measured at room temperature. In each of the L_2 and L_3 as well as the M_4 and M_5 spectra, two separate peaks,

~10 eV apart, are observed that reflect the nature of the 4*f* configuration as a result of final-state effects. This spectral signature shows that the Ce 4*f* configuration is α-phase-like.[17] The gradual intensity reduction of the peak at higher photon energy (labeled $4f^0$ in Fig. 2, see below) as Ce is increasingly substituted by Si implies a modification of the 4*f* configuration. The 4*f*-related final-state effects lead to a two-step profile in the L_1 spectrum (Fig. 2), which involves a transition into the unoccupied Ce 6*p*-derived valence states. Much effort has been devoted to study the final-state features in such spectra, with the aim to determining the ground-state properties. One of the central parameters in the description of this class of compounds is the effective 4*f*-state occupancy, n_{4f}. Since the $M_{4,5}$-edge spectroscopy is based on the transition of an electron into a 4*f* level it probes the 4*f* configuration, hence n_{4f}, in the ground state obviously more directly than the $L_{2,3}$-edge spectroscopy, in which it is involved only indirectly as a result of a final-state effect due to the 4*f*-electron 2*p*-core-hole interaction.[34,35] However, traditionally, this latter spectroscopy has been more frequently applied, and here we essentially focus on the study of the L_2 and L_3 edges.

1. Deconvolution of the $L_{2,3}$-edge spectra of Ce in the multilayers

The presence of a core hole in the XAS final state makes it difficult to quantitatively extract the ground-state 4*f* occupation number n_{4f} directly from the $L_{2,3}$-edge XAS data.[35,36] To get an estimate of this number for the $Ce_{1-x}Si_x$/Fe multilayers and of its variation with the Si concentration, we use a phenomenological approach[35] widely employed by experimentalists (see, e.g., Ref. 6). The two-peak structure of the L_2- and L_3-edge signatures (Fig. 2, bottom panel) is interpreted as a superposition of two "white-line" resonances associated with the final states $|2\underline{p}4f^1\underline{v}^{n+1}\rangle$ (main peak) and $|2\underline{p}4f^0\underline{v}^{n+2}\rangle$ (peak at higher energy). These features are superposed to a steplike absorption increase associated with an excitation into continuum states. The 4*f* ground-state occupancy n_{4f} then is simply obtained from the relative intensity of the two white lines; their width 2Γ correlates with the width of the Ce 5*d* band. For this purpose the spectra are deconvoluted by the superposition of two broadened Lorentzian functions and two arctangent step functions. Kotani and co-workers[37] and Malterre[38] have provided theoretical arguments that the $L_{2,3}$ near-edge absorption spectra of Ce yield a reliable image of its ground-state configuration. Hence, the phenomenological approach to the $L_{2,3}$ spectra, even if it is oversimplified, should provide a satisfactory measure of the 4*f* occupancy n_{4f} in the ground state, as long as the $|2\underline{p}4f^0\underline{v}^{n+2}\rangle$ signature has sufficient spectral weight.

The Ce 4*f* ground-state occupancy n_{4f} extracted from the L_2-edge spectra and the linewidth 2Γ, which is correlated with the width of the 5*d* band, are reported in Fig. 3 as a function of the Si concentration *x*. For $x \leqslant 0.1$, n_{4f} adopts the minimum value that is reached by α-Ce metal exposed to an external pressure.[39] Hence, Ce is in a phase with an α-like electronic configuration. With increasing *x*, there is a continuous increase of n_{4f} up to ~0.9. This reflects a *progressive reduction* of the 4*f*-state conduction-band hybridization, i.e.,

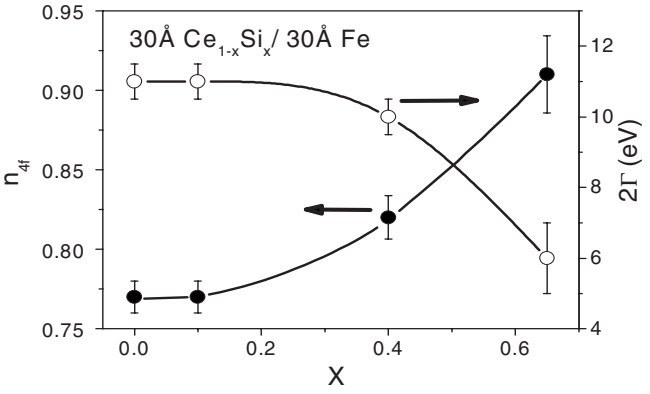

FIG. 3. Occupation of the Ce 4*f* states, n_{4f}, extracted from the analysis of the L_2 absorption edge (solid circles) for multilayers $Ce_{1-x}Si_x$ (30 Å)/Fe(30 Å) as a function of the Si concentration *x*. Also shown is the width of the "white lines" 2Γ resulting from the analysis of the L_2 edge (open circles).

an increasing degree of localization of the 4*f* states in the multilayers. The progressive decrease of the number of Ce neighbors apparently weakens the *f*-*d* hybridization in the alloy sublayers. At the highest Si content, $x=0.65$, n_{4f} approaches that of the γ-like Ce phase which is close to 1. This is corroborated by the evolution of the linewidth 2Γ which decreases from above 10 eV expected for α-like Ce in these multilayers to 6 eV expected when the γ-like Ce phase is approached.[17]

The conclusions drawn from the Ce-$L_{2,3}$ absorption spectra are corroborated by the evolution of the Ce-$M_{4,5}$ spectra of the multilayers (Fig. 2, top panel). The two-peak structure of both the M_4 and M_5 resonances corresponds to the final states $|3d^9 4f^2 \underline{v}^n\rangle$ (main contribution) and $|3d^9 4f^1 \underline{v}^{n+1}\rangle$ (satellite at the high-photon-energy end); they are directly related to the initial states $|3d^{10}4f^1\underline{v}^n\rangle$ and $|3d^{10}4f^0\underline{v}^{n+1}\rangle$. This spectral shape differs from the $M_{4,5}$ resonances of typical γ-phase-like Ce systems.[40] In that case, they exhibit a fine structure arising from the exchange splitting of the $|3d^9 4f^2 \underline{v}^n\rangle$ final state, which is well described by an atomic multiplet calculation of this configuration.[41] This fine structure is smeared out here due to the substantial hybridization between the 4*f*- and conduction-electron states, which confirms the α-phase-like character of Ce.[42] It is worth mentioning that in the corresponding spectra of weakly hybridized bulk $CeSi_2$, this fine structure is still visible, in addition to a weak $4f^1$ final-state satellite above the main peak.[7] The theoretical description of the $M_{4,5}$ absorption thresholds in highly correlated Ce systems appears to be much clearer than that of the $L_{2,3}$ edges.[34,43] However, a simple deconvolution of the $M_{4,5}$ spectra as the one performed for the $L_{2,3}$ edges to extract a value of the ground-state occupancy n_{4f} may not be reliable. This is due to complications arising from the interaction between the $3d_{3/2}$ and $3d_{5/2}$ core holes. In fact, such estimation of n_{4f} from the relative weight of the $4f^1$ and $4f^0$ channel intensity contributions (Fig. 2) tentatively performed here leads to numbers that show the same trend in the variation with the Si content as the ones resulting from the $L_{2,3}$-edge profiles but are systematically shifted to lower values. This is a similar observation as in a previous study.[17]

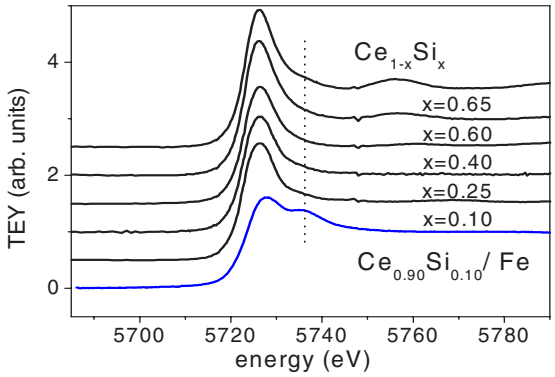

FIG. 4. (Color online) X-ray absorption spectrum at the Ce-L_3 edge of 500 Å thick $Ce_{1-x}Si_x$ films with different Si concentrations (total-electron-yield detection) and of a multilayer $Ce_{0.9}Si_{0.1}$(30 Å)/Fe(30 Å) as a reference (bottom curve).

2. *Single* $Ce_{1-x}Si_x$ *alloy films*

The electronic ground-state configuration of Ce is different in single alloy films $Ce_{1-x}Si_x$. This is visible in the Ce-L_3-edge absorption spectra presented in Fig. 4 which confirms previous observations.[14] In contrast to the multilayers, essentially only a single white-line resonance is observed already at $x=0.1$. This means that here Ce is in the weakly hybridized γ-phase-like configuration. Apparently, the intercalation of $Ce_{1-x}Si_x$ between Fe in the multilayers stabilizes the α-like Ce configuration to a considerably high Si concentration. As suggested for the pure Ce/Fe multilayers,[18] this may be due to mismatch-related strain at the interfaces.

For the single alloy films in Fig. 4, the amplitude of the white line increases by about 35% as the Si concentration is raised to $x=0.65$. This visualizes a change in the electronic structure, presumably a charge transfer from the Ce 5*d* band to the *s*-*p* orbitals of Si. It can be seen in Fig. 4 that with increasing Si concentration, an oscillation appears in the spectra above the absorption edge beyond 5750 eV. This fine structure [near-edge x-ray absorption fine structure (NEXAFS)] is present in the spectra of the multilayers as well and indicates a structural change in the Ce environment on the scale of the atomic distances as it occurs when the number of Ce neighbors is reduced. Amorphous films of composition $Ce_{0.33}Si_{0.67}$ present a limit in this context since in this case, as was previously shown, each Ce ion is surrounded by 12 Si nearest neighbors.[16]

B. X-ray absorption magnetic circular dichroism spectroscopy

An important result of the previous study on Ce/Fe multilayers is that the Ce atoms in their α-phase-like electron configuration carry ordered magnetic moments of 5*d* and 4*f* origin due to interfacial interaction with Fe.[17–19] The 5*d* moment extends on a depth scale of at least 15 Å into the Ce layers and is coupled antiparallel to the Fe moment;[17,18] the 4*f* moment, equally antialigned to that of Fe, resides closer to the interface.[17]

The multilayers considered here belong to the class of systems combining rare earths (REs) with magnetic transition metals (TMs). The electronic and magnetic structure of bulk compounds of such elements may be theoretically described by a model of Brooks and Johansson;[44] according to general arguments, the underlying mechanisms may be applied to interface magnetism of the corresponding multilayers.[45] What is relevant here is that *hybridization between the itinerant RE 5d states and the spin-split TM 3d states*, with different strengths for the spin-up and spin-down states,[44] gives rise to an ordered 5*d* spin moment in the paramagnetic RE layers near the interface on a sizable depth scale oriented antiparallel to that of the TM 3*d* moment. Ordered magnetism on the RE 4*f* electrons originates from interactions with their electronic environment according to mechanisms *dissimilar* in the case of localized and itinerant 4*f* states. We briefly note that in the former case, magnetic order on the 4*f* electrons results from their intra-atomic exchange coupling with the magnetically polarized 5*d* electrons. This is realized in Ce systems with a γ-phase-like electronic configuration, such as in the multilayers $CeH_{2-\delta}$/Fe,[23,24] for example. The latter case, realized in α-phase-like Ce systems such as the intermetallic $CeFe_2$,[46–48] is more complex: the itinerant 4*f* states participate in band formation. In addition to 5*d*-3*d* hybridization now 4*f*-3*d* hybridization becomes important; it generates an induced 4*f* spin moment on Ce.[44] Applied to the present multilayer system, a gradual transition between these two cases is to be expected as n_{4f} is varied together with the Si concentration.

$L_{2,3}$*-edge XMCD spectra of Ce: Influence of the* 4*f magnetic moment on the dichroic shape*

It is essential to note that in all of these (bulk and layered) RE-TM systems, the RE 5*d* band states are a central issue in understanding the magnetic properties. XMCD spectra at the RE $L_{2,3}(2p)$ edges are an important tool for obtaining information on the 5*d*-electron magnetism, which is difficult to acquire separately by other methods. Figure 5 displays the L_2 and L_3 XMCD spectra of Ce in the $Ce_{1-x}Si_x$ multilayer sublayers for different Si concentrations at 300 and 10 K. As a signature of the 4*f* configuration mixing, each spectrum consists of two contributions, as the isotropic absorption spectrum (Fig. 2), with roughly the same splitting ($\sim$10 eV) of the $4f^1$ and $4f^0$ channels. Except for the sample with the highest Si content $x=0.65$ at 10 K, the signals are negative at the L_2 and positive at the L_3 edge. These signs indicate antiparallel orientation of the Ce 5*d* and Fe 3*d* magnetic moments for the definition of the XMCD signals employed here (Sec. II).[18] At the Ce L_1 edge (transition $2s \rightarrow 6p$), magnetic dichroism could not be detected despite the possibility of a magnetic polarization transfer to the 6*p* states by hybridization with the spin-split 5*d* states. In the light of a naive expectation, in a single particle description[49] the evolution of the dichroic L_2 and L_3 signals with Si concentration and temperature is largely anomalous. This is visible, for example, in the variation of the ratio of the XMCD signal amplitudes, L_2/L_3, shown in the inset of Fig. 5. An exception is the case with the lowest Si concentration $x=0.1$. Here, the XMCD signals increase when the temperature is reduced from 300 to 10 K, while the spectral shape is preserved. Furthermore, at both temperatures, as for the the Si-free multilayer ($x=0$), the ratio of the XMCD signal amplitudes, $|L_2/L_3|$, is

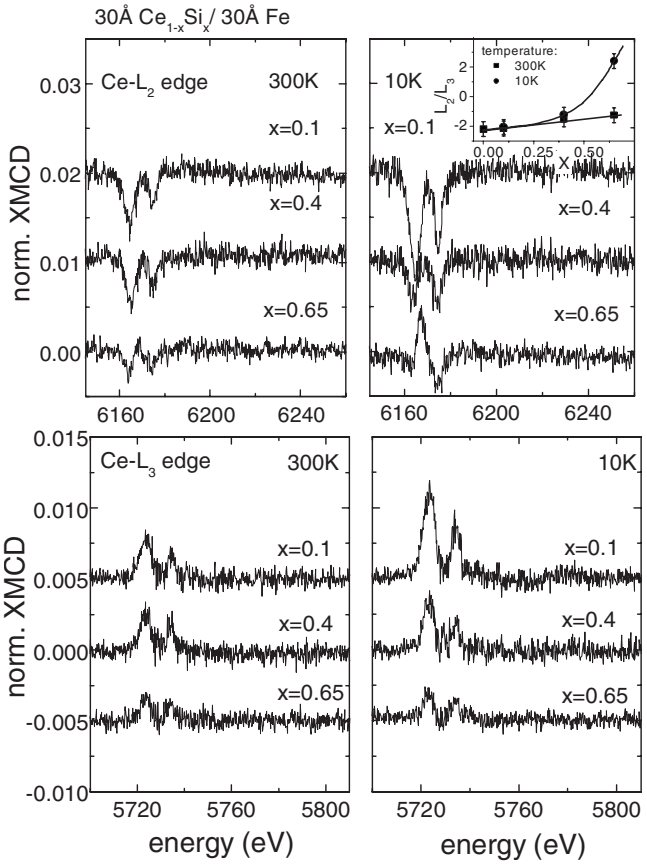

FIG. 5. XMCD spectra at the L_2 edge (top) and L_3 edge (bottom) of Ce for the multilayers $Ce_{1-x}Si_x/Fe$ with different Si concentrations x measured at 300 K (left) and 10 K (right). The spectra are normalized to a jump of 1 at both absorption edges and scaled to 100% x-ray polarization. Inset: Ratio of the amplitudes of the L_2- and L_3-edge XMCD signals (low-energy peaks), L_2/L_3. The values must be divided by 2 to take the different degeneracy of the spin-orbit split $2p$ core states into account (see text).

close to the statistical value of 1. This is imposed by the degeneracy of the $2p_{1/2}$ and $2p_{3/2}$ core states, in a simple picture of the $2p \rightarrow 5d$ dipole transition, with negligible spin-orbit coupling in the $5d$ final state.[50] The values shown in the inset of Fig. 5 are based on the equal normalization of the XA spectra at both edges, L_2 and L_3. They must be divided by 2 if the different heights of the two absorption edges, imposed by the core-state degeneracy, are taken into account. This behavior reproduces the previous observations on the Ce/Fe multilayers; it shows that the orbital contribution to the $5d$ magnetic moment is almost zero, i.e., the moment is essentially of pure spin origin.[18] This is a manifestation of crystal-field effects which are commonly expected to quench the orbital moment of d-band electrons. It can be seen in Fig. 5 that the situation is different for the other multilayers more rich in Si, $x > 0.1$. At 300 K, the amplitudes of the dichroic signals at both the L_2 and L_3 edges decrease monotonously with growing Si concentration, while the spectral shape does not change. This decrease mirrors, as we shall argue below, a progressive strengthening of the $4f$-$5d$ exchange interaction. The evolution of the XMCD spectra appearing when the temperature is reduced to 10 K is intriguing. For a given Si concentration $x > 0.1$, the amplitudes do not simply grow. At the L_2 edge (Fig. 5, top), the spectral shape changes, most dramatically for $x = 0.65$ where it is derivativelike owing to the reversed sign of the low-energy peak related to the $4f^1$ channel. In contrast, the shape of the L_3-edge spectra (Fig. 5, bottom) is essentially preserved. A further fingerprint of these spectral anomalies at $x > 0.1$ is the deviation of the ratio XMCD amplitudes ratio, $|L_2/L_3|$, from the statistical value of 1 (Fig. 5, inset).

The complex XMCD spectrum at the Ce-L_2 edge of the multilayer $Ce_{0.35}Si_{0.65}/Fe$ at 10 K is similar to the Ce L_2-edge dichroic spectra of the multilayers $CeH_{2-\delta}/Fe$ (Ref. 27) which have a γ-phase-like Ce $4f$ configuration. This suggests that the increased localization of the Ce $4f$ states in the Si-rich $Ce_{0.35}Si_{0.65}$ sublayer plays a role in the anomaly. Let us note that in the hydride multilayer system, the shape and the amplitude of the XMCD signals vary strongly with the angle between the magnetic field, which is parallel to the beam, and the layer normal. The effect is related to the magnetocrystalline anisotropy of the multilayers which induces a perpendicular magnetization orientation at low temperatures.[24] No anisotropy in the Ce-L-edge XMCD spectra in any of the $Ce_{1-x}Si_x/Fe$ multilayers could be detected,[51] in agreement with the observation that its global magnetization lies in the layer plane at all temperatures.

In spite of their importance, it is not straightforward to draw instructive information from the experimental XMCD spectra at the RE $L_{2,3}(2p)$ edges.[52] In fact, interpretation of these spectra is a matter of discussion since their first publication.[53] For example, they do not simply provide information on the spin-resolved $5d$ density of states; even the sign of XMCD intensities could not be predicted by a basic theory. Complexities arise from the intra-atomic exchange interaction between $5d$ and $4f$ electrons, which leads to a spin-dependent enhancement of the $2p$-$5d$ radial matrix element in the photoabsorption process.[54] It means that the L-edge XMCD depends on the $4f$ states. Model calculations considering the $5d$-$4f$ exchange interaction[55–57] have shown that it is indispensable for a proper interpretation of the spectra; it is differently effective at the L_2 and L_3 edges. The calculations were successful, for example, in describing basic trends in the signs and widely varying ratios of dichroic signals in RE-based intermetallics.[52] Nevertheless, in spite of these achievements and more recent theoretical progress[48] understanding of these spectra remains limited to date.

Since a rigorous theoretical description of the RE-$L_{2,3}$-edge dichroism does not exist, we use a physically transparent phenomenological procedure to model the evolution of the Ce-$L_{2,3}$ XMCD spectra of the $Ce_{1-x}Si_x/Fe$ multilayers with the Si content and temperature. It is motivated by and based on the existing model calculations of dichroic $L_{2,3}$-edge spectra of RE[56,57] and makes use of the method[35] applied above to analyze the isotropic XAS spectra at the $L_{2,3}$ edges of the RE (Sec. III A). Previously invoked to analyze the $L_{2,3}$ XMCD spectra of Ce in the $CeH_{2-\delta}/Fe$ multilayers, it has led to basic insights concerning the spectral shape and intensity related to the underlying physical mechanisms.[27] We assume that the magnetic interaction of the RE $5d$ states with Fe at the interfaces in the multilayers has two effects that control the $L_{2,3}$ XMCD spectra of the

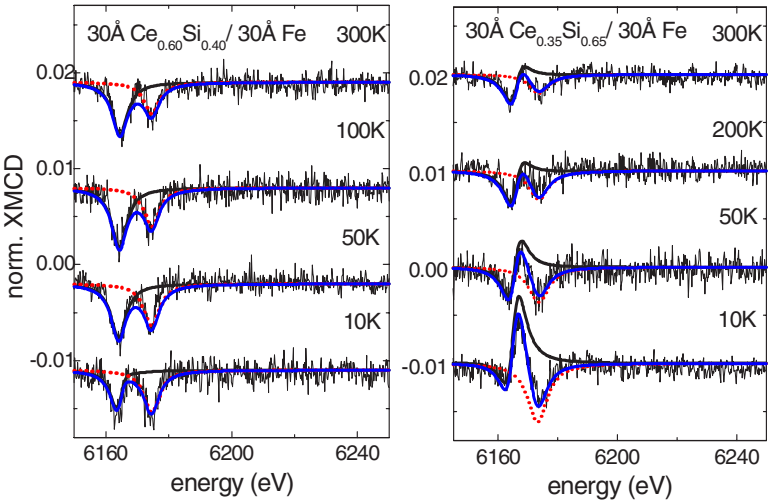

FIG. 6. (Color online) Analysis of the L_2-edge XMCD spectra of Ce in two multilayers $Ce_{1-x}Si_x$/Fe with 40% (left) and 65% Si (right) at different temperatures using the model described in the text [Eqs. (1)–(3)]. Shown are the fit for the first transition ($4f^1$ channel) at lower photon energy (black continuous line, yielding the parameters α and β), the transition at higher energy [$4f^0$ channel, red (dotted) line], and their sum [blue (continuous) line].

RE; they are represented by two parameters, α and β. (The model is only briefly addressed here. For a more detailed discussion, see Ref. 27).

(i) The interfacial interaction results in a difference in the spectral weight for unoccupied spin-up and spin-down $5d$ states that may be ascribed to an *effective magnetic polarization*,

$$\alpha = (\Delta\rho/\rho + \Delta M/M). \tag{1}$$

It determines the dichroic intensity corresponding to the $2p \rightarrow 5d$ electric dipole (E_1) transition, in an extension of an independent particle description,[53,58] by

$$\Delta\mu = P_e\alpha, \tag{2}$$

where $\Delta\mu$ is normalized to the isotropic absorption coefficient (Sec. II). The relation combines the difference of unoccupied spin-up (majority) and spin-down (minority) $5d$ states per atom in the ground state, $\Delta\rho = \rho^{\uparrow} - \rho^{\downarrow}$, here induced by $5d$-$3d$ hybridization, and the difference between the radial parts of the matrix element for the transition to these states, $\Delta M = M^{\uparrow} - M^{\downarrow}$; ΔM results from the exchange interaction between the excited $5d$ electron and the $4f$ electron, $\varepsilon_{4f\text{-}5d}$, which generates a spin-dependent contraction ("breathing") of the radial part of the $5d$ wave function that is proportional to $\varepsilon_{4f\text{-}5d}$.[59] P_e is the spin polarization of the photoelectron (−0.5 and +0.25 for the L_2 and L_3 edges, respectively). For a net $5d$ magnetic moment oriented parallel to the x-ray propagation direction, we have $\Delta\rho < 0$ and $\Delta M > 0$. ($\Delta\rho$ is in the range of a few percent at the RE-$L_{2,3}$ edges, whereas ΔM can rise to 20%–30%.[58]) Hence, due to the different sign of $\Delta\rho$ and ΔM, an enhancement of $M^{\uparrow}$ may reverse the sign of the XMCD signal [Eq. (2)]. Equation (1) mixes band-structure effects ($\Delta\rho$) and intra-atomic final-state interaction (ΔM). In spite of its intra-atomic character, it should be a good approximation for metallic systems due to the local nature of the $L_{2,3}$ XMCD.

(ii) There is a *splitting in energy* for the final states of the excited spin-up and spin-down $5d$ electron, we denote by β. One part of the effect is due to $4f$-$5d$ exchange interaction $\varepsilon_{4f\text{-}5d}$ (Refs. 56 and 57) as in the case of the parameter α, another part to the exchange interaction between the RE $5d$/Fe $3d$ hybridized final state and the $2p$ core hole.[60] Note that the parameters α and β are correlated due to their dependence on $\varepsilon_{4f\text{-}5d}$.

The two parameters α and β are used to model the $L_{2,3}$ XMCD intensity as a function of energy E by following the approach of Röhler[35] for the deconvolution of the x-ray absorption spectra at the RE $L_{2,3}$ edges (see Sec. III A). The white-line resonances for both spin channels in the E_1 transition to the spin-up and spin-down unoccupied $5d$ states are approximated by Lorentzian functions with an amplitude A_L and a width 2Γ their difference is used to represent the XMCD intensities at the L_3 edge (upper sign) and L_2 edge (lower sign):

$$\Delta\mu(E,A_L,2\Gamma) = \pm L(E,A_L,2\Gamma) \mp L(E-\beta,A_L(1-\alpha),2\Gamma+\beta). \tag{3}$$

The different signs express the opposite orientation of the spin of the photoexcited electron at the L_3 and L_2 edges. For a general discussion of the effect of the two parameters α and β in Eq. (3), see Ref. 27.

There is little doubt that the anomalies of the XMCD spectra at the $L_{2,3}$ edges of Ce addressed above (Fig. 5), such as the decrease in intensity with increasing Si content x or the change in shape with decreasing temperature (at $x > 0.1$) and the variation of the XMCD ratio L_2/L_3, can be attributed to the $5d$-$4f$ exchange interaction. Note that a growing Si content is accompanied by a growing $4f$-state occupancy n_{4f} (Fig. 3), i.e., by an increased localization of the Ce $4f$ states. We have analyzed the dichroic Ce-$L_{2,3}$-edge spectra of the $Ce_{1-x}Si_x$/Fe multilayers by the phenomenological model [Eq. (3)]. As an example, Fig. 6 shows the results for the L_2 edge, for two Si concentrations, $x = 0.4$ and 0.65, at various temperatures. Separate fits are applied for the XMCD signatures of the $4f^1$ channel at the absorption edge, using Eq. (2), and of the $4f^0$ channel at ~10 eV above the edge, using an additional Lorentzian function.[35] The results of the analysis of the white-line spectra were used as initial parameters (width 2Γ, amplitudes A_L, and the ratio of the $4f^1$ and $4f^0$ contributions); thus, only α and β and the polarization of the $4f^0$ contribution are used as free parameters. Inspection of Fig. 6 reveals that the evolution of the dichroic spectra with

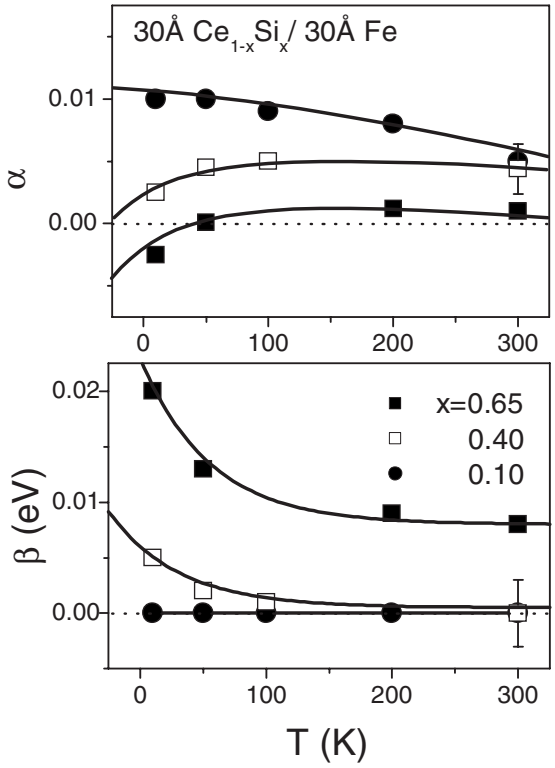

FIG. 7. Parameters α and β as a function of temperature resulting from the fits of the phenomenological model [Eqs. (1)–(3)] to the Ce-L_2-edge XMCD spectra of multilayers $Ce_{1-x}Si_x$/Fe with different Si concentrations x. Solid lines: Exponential functions serving as guides for the eye (see Ref. 51).

temperature lowered from 300 to 10 K is well described. In fact, the negative signal at the Ce L_2 edge results from Eq. (1) if $|\Delta M/M| < |\Delta\rho/\rho|$ and the projected Ce $5d$ magnetic moment is oriented opposite to the x-ray propagation direction, which is parallel to the external magnetic field. Since in the experiment the Fe magnetic moment is aligned along the field, this antiparallel moment orientation is an expectation of the band-structure theory of RE-TM compounds[44] addressed above. Note the decrease in amplitude of the $4f^1$ signal for $x=0.4$ (left panel) and the gradual variation of this feature from predominantly negative to strongly positive XMCD for $x=0.65$ (right panel). The values of the parameters α and β extracted from the analysis are presented in Fig. 7. The vanishing β for $x=0.1$ in the entire temperature range suggests that for this Si concentration, the $4f$-$5d$ exchange interaction is negligible. This is related to the important $4f$ valence-band hybridization in this case and means that the XMCD signal represents the spin polarization of the Ce $5d$ band in the ground state, i.e., $\alpha \approx (\Delta\rho/\rho)$. It is not surprising that we have $|L_2/L_3| \approx 1$ for the XMCD amplitude ratio, which is the statistical value. For $x=0.4$, a slight decrease of α at 10 K goes along with a finite β. It means that the $4f$-$5d$ exchange interaction is effective, hence the spin dependence of the matrix element for the $2p \rightarrow 5d$ transition, ΔM, that competes with the $5d$ spin polarization $\Delta\rho$ gains in importance; α is reduced [Eq. (1)]. The reduced amplitude of the $4f^1$-related signal in the XMCD spectrum (Fig. 6) is a consequence. For $x=0.65$, $4f$-$5d$ exchange is even more important. As an effect of a substantial ΔM contribution, α is very small at 300 K and changes sign near 50 K. As α crosses zero, i.e., for $|\Delta M/M| \approx |\Delta\rho/\rho|$, the $4f^1$-related XMCD signal becomes derivativelike, emphasizing the role of β growing toward low temperature. To conclude, the variation of the parameters α and β of our model with temperature and Si content (Fig. 7) extracted from a comparison with the XMCD spectra in Fig. 6 clearly shows the importance of the $4f$-$5d$ exchange interaction for the Ce-L_2 spectra of the $Ce_{1-x}Si_x$/Fe multilayers for high Si concentration and low temperature. It goes along with a high $4f$-state occupancy n_{4f} (Fig. 3), i.e., an increased localization of the Ce $4f$ states. In that sense, the similarities of the dichroic spectra of the multilayer $Ce_{0.35}Si_{0.65}$/Fe (Fig. 6) and the hydrided multilayers $CeH_{2-\delta}$/Fe where the Ce electron configuration is γ-phase-like[27] are not surprising. The experiments reveal that the strength of the $4f$-$5d$ exchange interaction can be controlled by varying the composition of the $Ce_{1-x}Si_x$ sublayers.

Inspection of Fig. 5 shows that the XMCD spectra at the L_3 edge of Ce are affected by the $4f$-$5d$ exchange interaction, too: their intensity, for example, decreases with increasing Si content. However, the spectral shape is not modified at low temperature. In particular, there is no sign reversal as in the L_2-edge spectrum at $x=0.65$ Si (Fig. 6). It indicates that the $4f$-$5d$ exchange is less effective at this absorption threshold, in agreement with our observation on the $CeH_{2-\delta}$/Fe multilayers[27] and theoretical prediction for the enhancement of the relevant dipole matrix element M.[48] The spectra can be fitted to our phenomenological model. This result is not presented here, since not much new information can be learned from this analysis.

IV. CONCLUSION

The present XAS study discloses the highly correlated nature of $Ce_{1-x}Si_x$ layers in a multilayer environment with Fe. Their properties are profoundly different from those of the compounds $CeSi_{2-\delta}$ and CeSi. We have demonstrated that the configuration of the $4f$ states of Ce in the layered structure may be tuned from delocalized at low Si content x to more localized at high x. This is visible in an increase of the $4f$-state occupancy. An important parameter is the hybridization of the $4f$ and conduction-band states. It changes from weak strength in the bare $Ce_{1-x}Si_x$ layers where the Si-derived 3p states must be implicated in the mixing process to higher strength in the multilayers where the Ce $5d$ and Fe $3d$ states are involved. Furthermore, it decreases in the multilayers with increasing Si concentration. The reduced $4f$ conduction-band hybridization favors the intra-atomic exchange interaction of the $4f$ electrons with the $5d$ electrons of Ce, spin split by the interaction with Fe.

These results highlight the unique possibility of XAS and XMCD spectroscopy, here in particular, on the $L_{2,3}$ absorption edges of Ce, to explore the electronic and magnetic properties of this element in the multilayers. It is shown that a physically transparent model permits one to parametrize

the $L_{2,3}$-edge XMCD spectra for which a rigorous theory awaits to be established. In spite of its simplicity, it permits to trace down trends in the variation of shape and intensity of the spectra with Si concentration and temperature to the $4f$-$5d$ exchange interaction which is well known to have a strong bearing on the L-edge XMCD of RE systems.[52,56,57]

ACKNOWLEDGMENTS

Special thanks are due to G. Krill, J. P. Kappler, E. Dartyge, and F. Baudelet at LURE in Orsay for stimulative discussions and support at the beamline. This work was performed under the auspices of the Deutsche Forschungsgemeinschaft within SFB 345.

*Author to whom correspondence should be addressed; mmuenze@gwdg.de

[1] D. C. Koskenmaki and K. A. Gschneidner, Jr., in *Handbook on the Physics and Chemistry of Rare Earths*, edited by K. A. Gschneidner, Jr. and L. Eyring (North-Holland, Amsterdam, 1978), Vol. I, p. 337.

[2] O. Eriksson, R. C. Albers, A. M. Boring, G. W. Fernando, Y. G. Hao, and B. R. Cooper, Phys. Rev. B **43**, 3137 (1991).

[3] B. Johansson, Philos. Mag. **30**, 469 (1974); D. Gustafson, J. McNutt, and L. O. Roellig, Phys. Rev. **183**, 435 (1969); U. Kornstädt, R. Lässer, and B. Lengeler, Phys. Rev. B **21**, 1898 (1980).

[4] See, for example, C. Giorgetti, S. Pizzini, E. Dartyge, A. Fontaine, F. Baudelet, C. Brouder, Ph. Bauer, G. Krill, S. Miraglia, D. Fruchart, and J. P. Kappler, Phys. Rev. B **48**, 12732 (1993); L. Nordström, O. Eriksson, M. S. S. Brooks, and B. Johansson, *ibid.* **41**, 9111 (1990).

[5] D. Malterre, M. Grioni, and Y. Baer, Adv. Phys. **45**, 299 (1996), and references therein.

[6] C. Grazioli, Z. Hu, M. Knupfer, G. Graw, G. Behr, M. S. Golden, J. Fink, H. Giefers, G. Wortmann, and K. Attenkofer, Phys. Rev. B **63**, 115107 (2001).

[7] B.-H. Choi, R.-J. Jung, S.-J. Oh, E.-J. Cho, T. Iwasaki, A. Sekiyama, S. Imada, S. Suga, T. Muro, and Y. S. Kwon, J. Electron Spectrosc. Relat. Phenom. **136**, 15 (2004).

[8] K. Mimura, T. Takase, H. Mizohata, Y. Taguchi, K. Ichikawa, Y. Takeda, M. Arita, K. Shimada, H. Namatame, S. Noguchi, K. Okuda, M. Taniguchi, and O. Aita, J. Electron Spectrosc. Relat. Phenom. **114-116**, 723 (2001); K. Mimura, Y. Watanabe, H. Mizohata, K. Ichikawa, Y. Taguchi, O. Aita, A. Yamasaki, A. Sekiyama, S. Suga, T. Oguchi, S. Noguchi, O. Sakai, and T. Muro, Physica B **351**, 295 (2004); K. Mimura, S. Noguchi, M. Suzuki, M. Higashiguchi, K. Shimada, K. Ichikawa, Y. Taguchi, H. Namatame, M. Taniguchi, and O. Aita, J. Electron Spectrosc. Relat. Phenom. **144-147**, 715 (2005).

[9] H. Yashima, T. Sato, and K. Kohn, Solid State Commun. **43**, 193 (1982).

[10] S. A. Shaheen, Phys. Rev. B **36**, 5472 (1987); J. Appl. Phys. **63**, 3411 (1988).

[11] S. Doniach, Physica B & C **91**, 213 (1977).

[12] W. H. Lee, R. N. Shelton, S. K. Dhar, and K. A. Gschneidner, Jr., Phys. Rev. B **35**, 8523 (1987).

[13] T. Takahashi, T. Morimoto, T. Yokoya, M. Kohgi, and T. Satoh, Phys. Rev. B **49**, 15688 (1994).

[14] D. Malterre, G. Krill, J. Durand, G. Marchal, and M. F. Ravet, Phys. Rev. B **34**, 2176 (1986).

[15] D. Malterre, G. Krill, J. Durand, and G. Marchal, J. Phys. (Paris) **46**, C8-199 (1985).

[16] T. Hihara, K. Sumiyama, H. Yamaguchi, Y. Homma, T. Suzuki, and K. Suzuki, J. Phys.: Condens. Matter **5**, 8425 (1993).

[17] M. Arend, M. Finazzi, O. Schutte, M. Münzenberg, A.-M. Dias, F. Baudelet, Ch. Giorgetti, E. Dartyge, P. Schaaf, J.-P. Kappler, G. Krill, and W. Felsch, Phys. Rev. B **57**, 2174 (1998).

[18] F. Klose, O. Schulte, F. Rose, W. Felsch, S. Pizzini, C. Giorgetti, F. Baudelet, E. Dartyge, G. Krill, and A. Fontaine, Phys. Rev. B **50**, 6174 (1994).

[19] M. Finazzi, F. M. F. de Groot, A.-M. Dias, B. Kierren, F. Bertran, Ph. Sainctavit, J.-P. Kappler, O. Schulte, W. Felsch, and G. Krill, Phys. Rev. Lett. **75**, 4654 (1995).

[20] L. Sève, N. Jaouen, J. M. Tonnerre, D. Raoux, F. Bartolomé, M. Arend, W. Felsch, A. Rogalev, J. Goulon, C. Gautier, and J. F. Bérar, Phys. Rev. B **60**, 9662 (1999); N. Jaouen, J. M. Tonnerre, D. Raoux, E. Bontempi, L. Ortega, M. Münzenberg, W. Felsch, A. Rogalev, H. A. Dürr, E. Dudzik, G. van der Laan, H. Maruyama, and M. Suzuki, *ibid.* **66**, 134420 (2002).

[21] Ph. Bauer, F. Klose, O. Schulte, and W. Felsch, J. Magn. Magn. Mater. **138**, 163 (1994).

[22] R. Hassdorf, M. Grimsditch, W. Felsch, and O. Schulte, Phys. Rev. B **56**, 5814 (1997).

[23] O. Schulte, F. Klose, and W. Felsch, Phys. Rev. B **52**, 6480 (1995).

[24] M. Arend, W. Felsch, G. Krill, A. Delobbe, F. Baudelet, E. Dartyge, J.-P. Kappler, M. Finazzi, A. San Miguel-Fuster, S. Pizzini, and A. Fontaine, Phys. Rev. B **59**, 3707 (1999).

[25] W. Lohstroh, O. Schulte, W. Felsch, F. Klose, H. Maletta, H. Lauter, and G. P. Felcher, J. Magn. Magn. Mater. **210**, 357 (2000).

[26] S. S. Dhesi, H. A. Dürr, M. Münzenberg, and W. Felsch, Phys. Rev. Lett. **90**, 117204 (2003).

[27] M. Münzenberg, F. Leuenberger, W. Felsch, G. Krill, T. Neisius, S. Pascarelli, and S. Pizzini, Phys. Rev. B **67**, 224431 (2003).

[28] See, for example, the study of resonant photoemission of Ce/Fe(100) interfaces by N. Witkowski, F. Bertran, T. Gourieux, B. Kierren, D. Malterre, and G. Panaccione, Phys. Rev. B **56**, 12054 (1997).

[29] L. G. Parratt, Phys. Rev. **95**, 359 (1954); L. Nevot and P. Croce, Rev. Phys. Appl. **15**, 761 (1980).

[30] J. Thiele, F. Klose, A. Schurian, O. Schulte, W. Felsch, and O. Bremert, J. Magn. Magn. Mater. **119**, 141 (1993).

[31] J. Hesse and A. Rübartsch, J. Phys. E **7**, 526 (1974); G. Le Caer and J. M. Dubois, *ibid.* **12**, 1083 (1979).

[32] F. Baudelet, E. Dartyge, A. Fontaine, C. Brouder, G. Krill, J.-P. Kappler, and M. Piecuch, Phys. Rev. B **43**, 5857 (1991); F. Baudelet, C. Brouder, E. Dartyge, A. Fontaine, J.-P. Kappler, and G. Krill, Europhys. Lett. **13**, 751 (1990).

[33] D. Lefèbvre, Ph. Sainctavit, and C. Malgrange, Rev. Sci. Instrum. **65**, 2556 (1994).

[34] O. Gunnarsson and K. Schönhammer, in *Handbook on the Physics and Chemistry of Rare Earths*, edited by K. A. Gschneidner,

Jr., L. Eyring, and S. Hüfner (North-Holland, Amsterdam, 1987), Vol. 10, p. 103.
[35] J. Röhler, in *Handbook on the Physics and Chemistry of Rare Earths* (Ref. 34), p. 453.
[36] O. Gunnarsson and K. Schönhammer, Phys. Rev. B **28**, 4315 (1983); O. Gunnarsson, K. Schönhammer, J. C. Fuggle, F. U. Hillebrecht, J.-M. Esteva, R. C. Karnatak, and B. Hillebrandt, *ibid.* **28**, 7330 (1983).
[37] T. Jo and A. Kotani, Solid State Commun. **54**, 451 (1985); A. Kotani, J. Phys. (Paris) **48**, C9-869 (1987); A. Kotani and J. C. Parlebas, Adv. Phys. **37**, 37 (1988).
[38] D. Malterre, Phys. Rev. B **43**, 1391 (1991).
[39] J. Röhler, in *EXAFS and Near Edge Structure III*, edited by K. O. Hodgson, B. Hedman, and J. E. Penner-Hahn (Springer, Berlin, 1984), p. 679; J. Röhler, J.-P. Kappler, and G. Krill, Nucl. Instrum. Methods Phys. Res. **208**, 647 (1983).
[40] J. Ph. Schillé, F. Bertran, M. Finazzi, Ch. Brouder, J. P. Kappler, and G. Krill, Phys. Rev. B **50**, 2985 (1994).
[41] B. T. Thole, G. van der Laan, J. C. Fuggle, G. A. Sawatzky, R. C. Karnatak, and J.-M. Esteva, Phys. Rev. B **32**, 5107 (1985).
[42] T. Jo and A. Kotani, Phys. Rev. B **38**, 830 (1988).
[43] J. C. Fuggle, F. U. Hillebrecht, J.-M. Esteva, R. C. Karnatak, O. Gunnarsson, and K. Schönhammer, Phys. Rev. B **27**, 4637 (1983).
[44] M. S. S. Brooks and B. Johansson, in *Handbook of Magnetic Materials*, edited by K. H. J. Buschow (North-Holland, Amsterdam, 1993), Vol. 7.
[45] A. M. N. Niklasson, B. Johansson, and H. L. Skriver, Phys. Rev. B **59**, 6373 (1999).
[46] A. Delobbe, A.-M. Dias, M. Finatzzi, L. Stichauer, J. P. Kappler, and G. Krill, Europhys. Lett. **43**, 320 (1998).
[47] O. Eriksson, L. Nordström, M. S. S. Brooks, and B. Johansson, Phys. Rev. Lett. **60**, 2523 (1988).
[48] I. Harada, K. Asakura, A. Fujiwara, and A. Kotani, J. Electron Spectrosc. Relat. Phenom. **136**, 125 (2004).
[49] P. Carra and M. Altarelli, Phys. Rev. Lett. **64**, 1286 (1990); P. Carra, B. N. Harmon, B. T. Thole, M. Altarelli, and G. A. Sawatzky, *ibid.* **66**, 2495 (1991).
[50] J. L. Erskine and A. Stern, Phys. Rev. B **12**, 5016 (1975).
[51] M. Münzenberg, Ph.D. thesis, Universität Göttingen, 2000.
[52] F. Baudelet, C. Giorgetti, S. Pizzini, C. Brouder, E. Dartyge, A. Fontaine, J. P. Kappler, and G. Krill, J. Electron Spectrosc. Relat. Phenom. **62**, 153 (1993).
[53] G. Schütz, M. Knülle, R. Wienke, W. Wilhelm, W. Wagner, P. Kienle, and R. Frahm, Z. Phys. B: Condens. Matter **73**, 67 (1988).
[54] B. N. Harmon and A. Freeman, Phys. Rev. B **10**, 1979 (1974); X. Wang, T. C. Leung, B. N. Harmon, and P. Carra, *ibid.* **47**, 9087 (1993); J. C. Lang, S. K. W. Kycia, X. D. Wang, B. N. Harmon, A. I. Goldman, D. J. Branagan, R. W. McCallum, and K. D. Finkelstein, *ibid.* **46**, 5298 (1992).
[55] T. Jo and S. Imada, J. Phys. Soc. Jpn. **62**, 3721 (1993).
[56] H. Matsuyama, I. Harada, and A. Kotani, J. Phys. Soc. Jpn. **66**, 337 (1997); H. Matsuyama, K. Fukui, H. Maruyama, I. Harada, and A. Kotani, J. Magn. Magn. Mater. **177-181**, 1029 (1998); H. Matsuyama, K. Fukui, K. Okada, I. Harada, and A. Kotani, J. Electron Spectrosc. Relat. Phenom. **92**, 31 (1998).
[57] M. van Veenendaal, J. B. Goedkoop, and B. T. Thole, Phys. Rev. Lett. **78**, 1162 (1997); J. Electron Spectrosc. Relat. Phenom. **86**, 151 (1997).
[58] J. C. Lang, X. D. Wang, V. P. Antropov, B. N. Harmon, A. I. Goldman, H. Wan, G. C. Hadjipanayis, and K. D. Finkelstein, Phys. Rev. B **49**, 5993 (1994).
[59] J. B. Goedkoop, A. Rogalev, M. Rogaleva, C. Neumann, J. Goulon, M. van Veenendaal, and B. T. Thole, J. Phys. IV **7**, C2–415 (1997).
[60] G. van der Laan, J. Phys.: Condens. Matter **9**, L259 (1997); Phys. Rev. B **55**, 8086 (1997).